

COLORING HOT-DIP GALVANIZATION OF STEEL SAMPLES IN INDUSTRIAL ZINC-MANGANESE BATHS

M. Godzák^a, G. Lévai^b, K. Vad^c, A. Csik^c, J. Hakl^c, T. Kulcsár^a, G. Kaptay^{a, b, d, *}

^aUniversity of Miskolc, Egyetemvaros, Miskolc, Hungary

^bBay Zoltan Ltd, BAY-ENG, Miskolc, Hungary

^cInstitute for Nuclear Research (MTA ATOMKI), Debrecen, Hungary

^dMTA ME Materials Science Research Group, Miskolc, Hungary

(Received 31 May 2017; accepted 17 August 2017)

Abstract

Colored hot dip galvanization of various steel samples was realized in an industrial bath containing 738 kg of a Zn-Mn liquid alloy at 450 °C. Zinc was alloyed in three steps to reach 0.1, 0.15 and 0.2 w% of Mn in liquid zinc, and galvanization of 9 different steel samples was performed in all three baths. The obtained colors change in the sequence blue – yellow – pink – green with increasing the Mn-content of the bath and with increasing the wall thickness of the steel samples. The results are analyzed by Glow-discharge optical emission spectroscopy (GD-OES) and Secondary Neutral Mass Spectrometry (SNMS) techniques. It is shown that depending on the Mn-content and on the wall thickness of the steel the samples are coated by MnO of various thicknesses (in the range between 30 – 230 nm). This layer forms when the samples are removed from the Zn-Mn bath into surrounding air, before the Zn-layer is solidified. Light interference on this thin MnO layer causes the colors of the galvanized coating. Different colors are obtained in different ranges of MnO thicknesses, in accordance with the laws of optics. The minimum Mn-content of liquid Zn is found as 0.025 ± 0.010 m/m% to ensure that the original outer ZnO layer on Zn is converted into the MnO layer. This minimum critical Mn-content is in agreement with chemical thermodynamics.

Keywords: Hot-dip galvanization; Zn-Mn bath; Light interference; MnO layer; Colored coating.

1. Introduction

Hot-dip galvanizing is one of the industrial processes ensuring corrosion protection of steel [1-9]. Not only corrosion protection, but also decorative issues are important [10-12]. These two requirements are reached at the same time, if coloring hot dip galvanization is performed [13-24]. During this process the zinc bath is alloyed by a transitional metal, having stronger affinity towards oxygen compared to zinc (even stronger oxide-forming elements, such as Al or Mg are usually excluded from the zinc bath). When the steel sample is removed from this alloyed zinc bath, its surface is coated by about 30 - 100 micron layer of the same Zn alloy. When the sample is removed to air, the alloying element is preferentially oxidized on its outer surface. Depending on the alloying element nature and content, temperature and solidification time of the Zn-coating, this top oxide layer grows to a certain

thickness, usually in the order of 50 – 200 nm. This transparent oxide layer provides a color to the coating due to interference of natural light.

Although the above process has been quite extensively studied in laboratory conditions [13-24], there are no reports on industrial tests. Thus, the goal of this paper is to fill this knowledge gap and to report on the results of our industrial trials of colored hot dip galvanization, using Zn-Mn alloys.

2. Materials and experimental details

For the experiments special high grade zinc (SHG-Zn) was used, alloyed by electrolytic manganese (Mn); their chemical compositions are given in Tables 1-2 measured by ICP (Inductive Coupled Plasma) Spectroscopy. Altogether 9 types of steel samples were used for galvanization, with their shapes, sizes and chemical compositions given in Table 3 (the latter was measured by Glow-discharge optical emission spectroscopy).

Dedicated to the memory of Professor Dragana Živković

* Corresponding author: kaptay@hotmail.com



Table 1. The chemical composition of SHG-Zn in m/m% (less than 0.0001 m/m% is found for Co, Cr, Fe, Mg, Mo, Ni, P, Ti, V)

Si	Al	Mn	Pb	Sn	B	S	Cd	Cu	Bi	Sb
0.0089	0.0054	0.0035	0.0023	0.0020	0.0014	0.0013	0.0004	0.0003	0.0002	0.0002

Table 2. The chemical composition of electrolytic Mn in m/m% (less than 0.0001 m/m% is found for Cd, Ti, V)

Mg	S	Si	Pb	Al	P	Zn	Cu	B	Ni	Bi
0.0136	0.0127	0.0075	0.0061	0.0059	0.0043	0.0038	0.0036	0.0022	0.0016	0.0009
Sb	Sn	Fe	Co	As	Cr	Sb				
0.0007	0.0007	0.0006	0.0004	0.0003	0.0002	0.0001				

Table 3. The shapes, sizes (mm) and the chemical compositions (m/m%) of steel samples

DC04 steel sheet 80×100×0.8									
C	P	S	Mn	Si	Cu	Cr	Ni	Al	
0.010	0.0070	0.0094	0.21	0.031	0.011	0.010	0.0025	0.025	
U-profile 30×15×2×190									
C	P	S	Mn	Si	Cu	Cr	Ni	Al	
0.076	0.0050	0.0047	0.38	0.10	0.017	0.027	0.022	0.041	
Hollow profile 1 40×20×2 ×250									
C	P	S	Mn	Si	Cu	Cr	Ni	Al	
0.084	0.0052	0.0026	0.62%	0.0024	0.12	0.072	0.036	0.055	
Hollow profile 2 40×40×3 ×250									
C	P	S	Mn	Cu	Cr	Ni	Al		
0.083	0.0049	0.0010	0.58	0.12	0.072	0.036	0.054		
Longitudinal welded pipe ø33×3 ×250									
C	P	Mn	Si	Cr	Ni	Al			
0.027	0.0030	0.18	0.0018	0.016	0.012	0.032			
Flat steel 1 50×4 ×250									
C	P	S	Mn	Si	Cu	Cr	Ni	Al	
0.081	0.0088	0.00050	0.38	0.0065	0.019	0.038	0.019	0.034	
Angle iron 50×50×5 ×60									
C	P	S	Mn	Si	Cu	Cr	Ni	Al	
0.056	0.023	0.023	0.62	0.27	0.49	0.15	0.15	0.0020	
Flat steel 2 50×10 ×250									
C	P	S	Mn	Si	Cu	Cr	Ni	Al	
0.079	0.0078	0.0022	0.49	0.0068	0.0079	0.0080	0.010	0.040%	
Cylinders ø80 ×30									
C	P	S	Mn	Si	Cu	Cr	Ni	Al	
0.046	0.0058	0.0041	0.49	0.18	0.25	0.10	0.12	0.044	

The initial amount of Zn in our industrial trials was 738 kg. Three cycles of Mn-alloying and hot dip galvanization were performed. In each alloying cycle 2.5 kg of Mn was alloyed in a cumulative way, so totally 7.5 kg of Mn was added to 738 kg of Zn. Electrolytic Mn is available in thin and small cathodic

plates, which “swim” on the oxidized surface of liquid zinc. That is why, to avoid excessive Mn-losses, the following alloying technology was followed: alloying was performed in silicon carbide (SiC) crucibles of A10 type. First, 4 kg of liquid Zn at 450 °C was added into this preheated crucible followed by the addition

of 2.5 kg of Mn plates at room temperature on its top, and finally the plates were covered by further 2 kg of liquid zinc with temperature of 450 °C. The content of the crucible was solidified within several minutes, so it could be removed from it. The resulting heterogeneous ingot of 8.5 kg was immediately added into the 730+ kg of liquid zinc bath. This ingot immersed under the surface of liquid zinc. The ingot fully dissolved in the large liquid Zn bath within 5 minutes. The bath was mixed for homogenization for further 20 minutes before sampling and galvanization was performed. Samples were taken from the homogenized Zn-Mn bath after each alloying / homogenization step and after each galvanization step. The resulting Mn-content of Zn as measured by ICP was about 0.10 m/m % (first cycle), 0.15 m/m% (second cycle) and 0.20 m/m% (third cycle). Thus, the alloying efficiency is found as about 30 % (first cycle) and about 15 % (second and third cycles). The Mn-content of the bath did not vary significantly between any two alloying cycles.

Galvanization was performed at the Tiszacsege (Hungary) plant of the NAGÉV Cink Ltd, where a commercial galvanizing container containing 800 tons of liquid zinc is used for industrial purposes. A smaller steel container 1 m long * 0.3 m wide * 0.7 m high was specially prepared for the present experiments. This container was filled with 738 kg of SHG-Zn and positioned on the top of the large industrial container perpendicular to its longer axes (see Fig.2). The zinc in our smaller container was kept by a gas burner at a constant temperature of 450 °C. The Zn in our smaller container reached the same temperature within 12 hours. Thus, the temperature of all experiments was fixed at 450 °C.

Before hot-dip galvanizing the steel samples, they were degreased by a Dexacid H420 solution, rinsed by tap water, then pickled in a 25-37 wt% HCl aqueous solution and rinsed by tap water again. After that the surface was fluxed by Fluorflux SPG aqueous solution (Fluorodienne Chimie S.A) and dried. Then, the samples were dried and pre-heated right above the

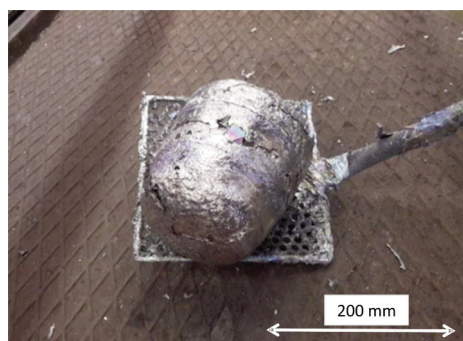


Figure 1. The Zn-Mn ingot obtained during the alloying of liquid Zn by Mn (this ingot was added into about 730+ kg of zinc bath, see Fig.2).

hot Zn-Mn alloy, using its waste heat. After 5 minutes of this pre-heating operation, the steel samples were immersed into the Zn-Mn liquid alloy for hot-dip galvanization. The velocity of immersion and removal was 50 mm/s. The time of immersion of each sample was 5 minutes. The 9 samples (in 3 parallel runs per cycle) were dipped together into the liquid bath, using an industrial crane (Fig.3). Care was taken to ensure that the samples do not touch each other or the wall of the container during immersion. Right before immersion and removal of the samples the oxide layer was mechanically removed from the surface (within a minute after surface oxide removal, the surface became coloured again due to fast thickening of the MnO layer – see Fig.3). All samples were removed from the bath into air. The average temperature in the industrial hall was about 5 °C (the experiments were performed on 4th January 2017, before starting the normal industrial operation by the plant for the year of 2017).

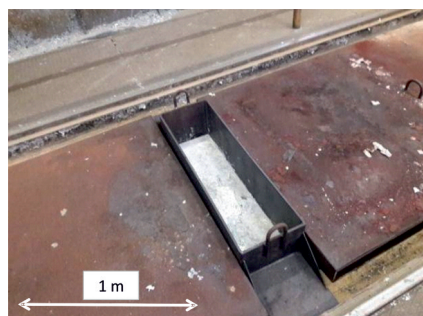


Figure 2. The container used by us containing 738 kg of liquid Zn, positioned perpendicular to the long axes of a large steel container (covered by steel plates during our experiments) containing 800 tons of liquid Zn kept at constant temperature of 450 °C



Figure 3. Samples hanging from a crane (not shown) above the liquid bath during the pre-heating period before their immersion (one can see the colors on the surface of the bath).

3. Experimental results

3.1. The observed colors of the samples as seen by human eye

The photographs of the different samples treated in the Zn-Mn baths of different Mn-contents are shown in Figs. 4-12. The same sample type treated in the three galvanizing cycles with three different Mn-contents in the bath are shown in the same figure for better comparison. The samples are shown in order of their increasing wall thickness values from Fig.4 (0.8 mm wall thickness) to Fig.12 (30 mm wall thickness). The summary of observed colors is given in Table 4. As follows from Table 4, the colors change in the sequence blue – yellow – pink – green with increasing the Mn-content of the bath and/or increasing the wall thickness of the steel samples.

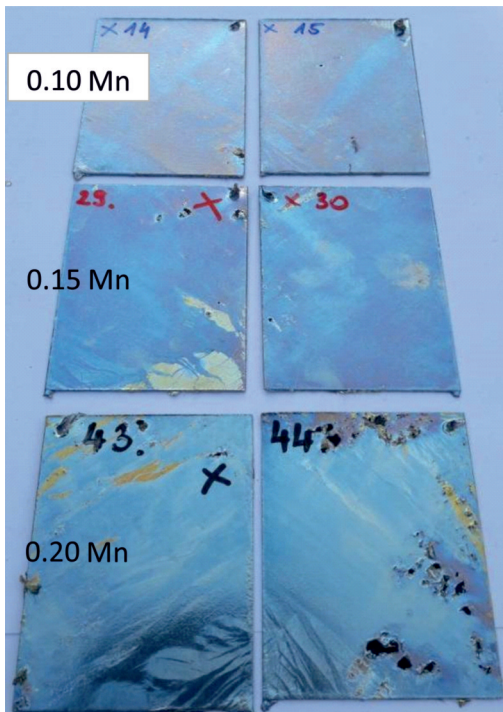


Figure 4. Photos of 80×100×0.8 mm steel plates treated in different baths (Mn contents are given in m/m%)

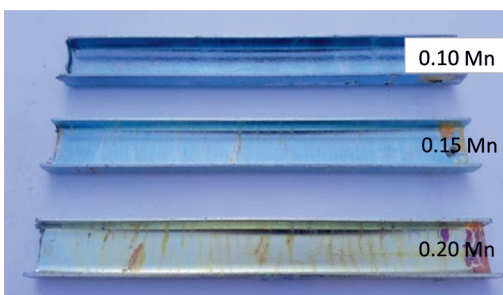


Figure 5. Photos of 30×15×2×190 mm U-profiles treated in different baths (Mn contents are given in m/m%)



Figure 6. Photos of 40×20×2×250 mm hollow profiles 1 treated in different baths (Mn contents are given in m/m%)

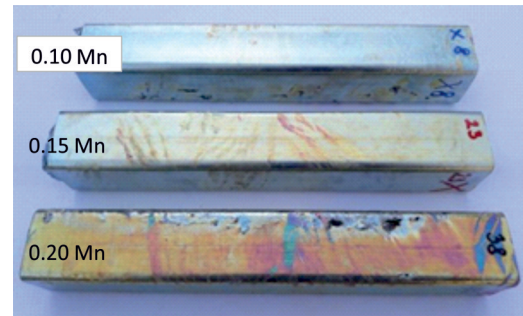


Figure 7. Photos of 40×40×3×250 mm hollow profiles 2 treated in different baths (Mn contents are given in m/m%)

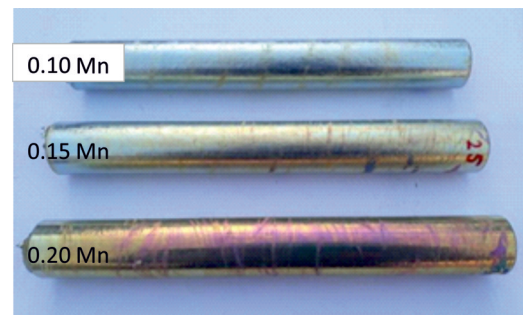


Figure 8. Photos of ø33×3×250 mm longitudinal welded pipes treated in different baths (Mn contents are given in m/m%)



Figure 9. Photos of 50×4×250 mm flat steel 1 samples treated in different baths (Mn contents are given in m/m%)

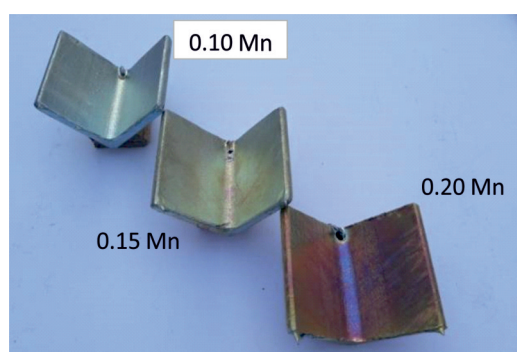


Figure 10. Photos of 50×50×5×60 mm angle iron samples treated in different baths (Mn contents are given in m/m%)

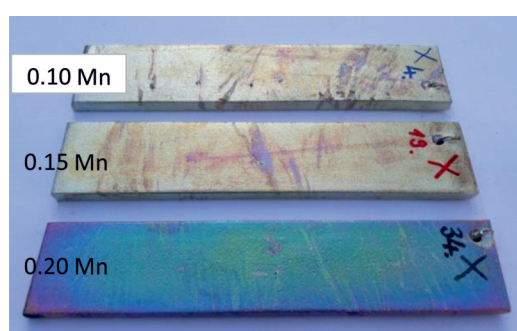


Figure 11. Photos of 50×10×250 mm flat steel samples 2 treated in different baths (Mn contents are given in m/m%)

3.2. The results of the GD-OES measurements

The characteristic GD-OES (Glow-discharge optical emission spectroscopy) spectra for different elements are shown for one of the samples (Fig.9, Mn-content: 0.20 m/m%) in Fig.13 in three different magnifications. The sub-figures in Fig.13 show the atomic % of different elements in the top layer of the sample as function of the depth measured from the outer surface. The following conclusions are drawn from Fig.13:

- the thickness of the Zn-Mn layer on the top of the steel sample can be estimated from the cross section

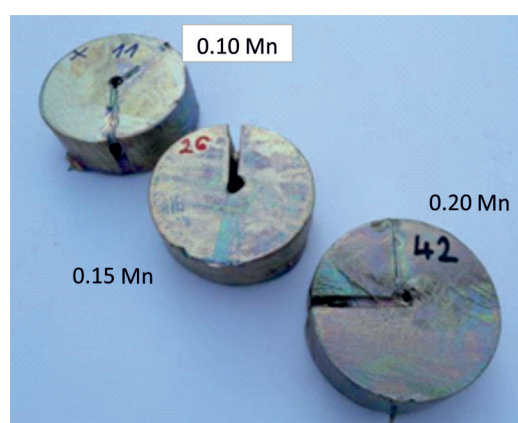


Figure 12. Photos of ø80×30 mm cylindrical samples treated in different baths (Mn contents are given in m/m%)

of the lines corresponding to the Zn-content and the Fe-content (see about 49 mm in top Fig.13). Plateaus are observed on both lines of Zn-content and Fe-content in top Fig.13 in the depth range between 20 – 40 mm correspond to an intermetallic compound formed between Zn and Fe. Thus, the majority of the thickness of the galvanized layer is made of a Zn-Fe intermetallic and not pure Zn (or Zn-Mn).

- as follows from middle Fig.13, the outer 25 – 125 nm layer of the sample is enriched in Mn. However, as our GD-OES was not able to detect oxygen, it is not clear from here in which form Mn is enriched on the surface. This question will be further discussed in the next sub-section.

- as follows from bottom Fig.13, the outermost layer of about 25 nm in thickness contains Si, Fe, Al and Mg, which are coming from Zn (Table 1), Mn (Table 2) and from the steel samples.

3.3. The results of SNMS measurements

A characteristic SNMS (Secondary Neutral Mass Spectrometry) profile of one of the samples is shown in Fig.14. Fig.14 basically shows the same information as Fig.13, but Fig.14 provides much higher resolution for all elements (including also

Table 4. The observed colors of the galvanized samples - see last three columns, as function of the Mn-content of the bath in m/m% (abbreviations: y = yellow, p = pink, g = green)

Fig	Shape	Size, mm	thickness, mm	0.10 Mn	0.15 Mn	0.20 Mn
4	plate	80*100	0.8	blue	blue	blue
5	U-profile	30*15*190	2	blue	blue	blue + y
6	hollow profile 1	40*20*250	2	blue	blue	blue + y
7	hollow profile 2	40*40*250	3	blue	blue + y	pink
8	pipe	ø30*250	3	blue	yellow	pink
9	flat 1	50*250	4	blue	blue + y	yellow
10	angle	50*50*60	5	blue	yellow	pink
11	flat 2	50*250	10	yellow	yellow + p	green
12	cylinder	ø80	30	yellow	yellow + g	pink + g

oxygen), measured for smaller depths from the outer surface. The most important information from Fig.14 is that the measured at% of Mn and at % of O are almost the same and are almost constant in the outer 50 - 175 nm of the sample. Thus, the dominating surface phase is MnO. Beyond the depth of 175 nm the sample is dominated by Zn. In the most outer layer (below 50 nm) the Mn-content is gradually decreased and is replaced by contaminant elements, such as Fe, Si, Al and Mg (Mg is detected, but its concentration is below the level shown in Fig.14; the contamination originates from Zn and Mn - see Tables 1-2 - and from the steel samples). However, the total outer layer of 175 nm is composed of oxides, dominated by MnO. All this is in agreement with Fig.13, but compared to Fig.13 more details are revealed. Most importantly it

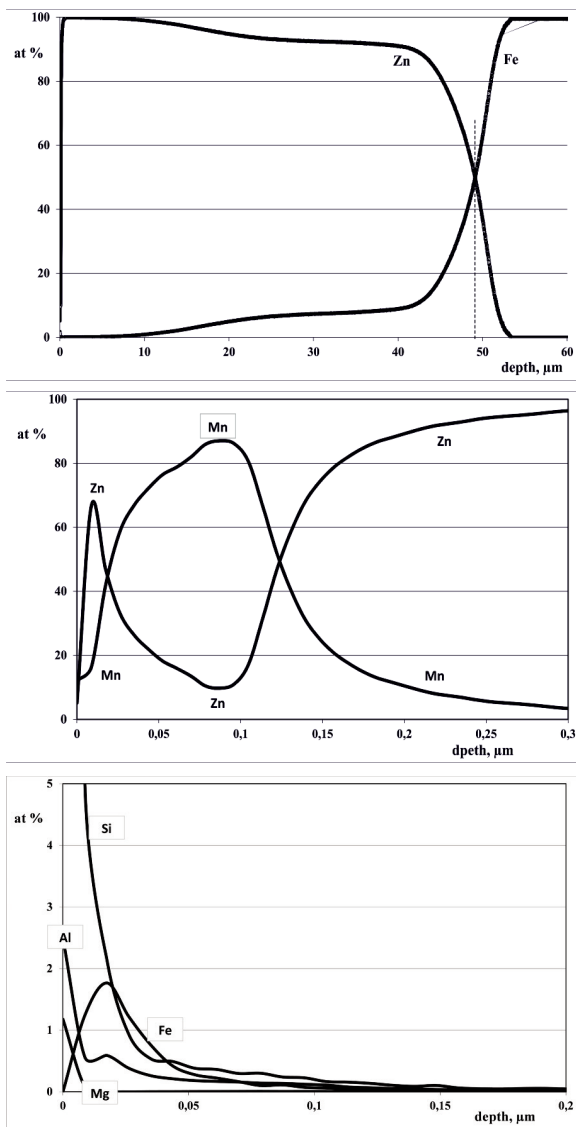


Figure 13. GDOES spectrum of the sample Fig.9/0.2, shown in 3 different magnifications

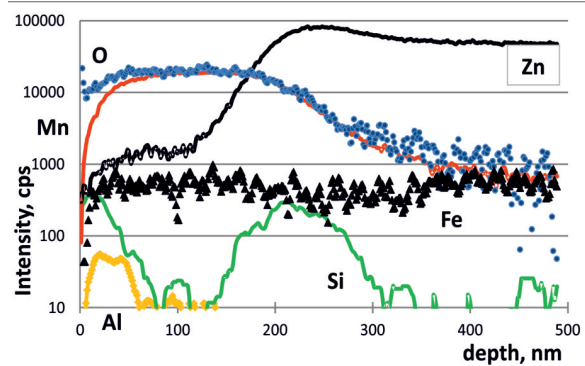


Figure 14. A characteristic SNMS spectrum of one of the samples (Fig.10, 0.2 m/m% Mn). The y-axis is proportional to the at% of the elements. The dotted vertical line corresponds to the thickness of the outer oxide layer, which is mainly MnO. black line: Zn; blue dots: O; red line: Mn, black triangles: Fe, green line: Si, orange diamonds: Al.

is clear now that the outer layer of the sample is made of oxides, with a dominating MnO phase.

In Fig.15 the dependence of the thickness of the outer oxide layer is shown as function of the wall thickness of the steel samples at two different Mn-contents of the Zn-bath. One can see that the measured by SNMS MnO-thickness values increase with both Mn-content of the bath and wall thickness of the steel samples.

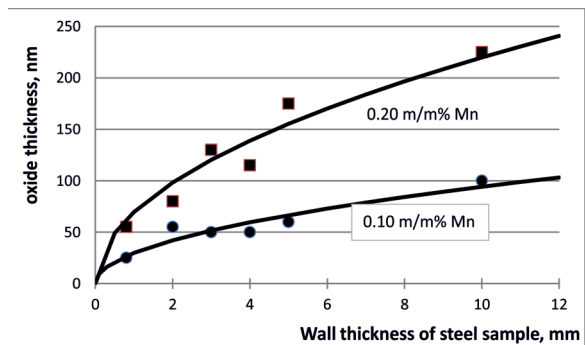


Figure 15. The thickness of the outer oxide layer as function of the Mn-content of Zn and wall thickness of the steel samples. Points: measured values by SNMS (squares: 0.20 m/m% Mn, circles: 0.10 m/m% Mn), lines calculated by Eq.(1)

4. Discussion

4.1. Modelling the thickness of the MnO layer

Using the measured data of Fig.15, the following semi-empirical relationship is found between the thickness of the MnO layer (d_{MnO} in nm), the Mn-content of the Zn-bath ($C_{(Mn(Zn))}$ in m/m%) and the wall

thickness of the steel samples (d_{Fe} in mm):

$$d_{MnO} \cong (397 \pm 30) \cdot (C_{Mn(Zn)} - (0.025 \pm 0.010)) \cdot \sqrt{d_{Fe}} \quad (1)$$

As follows from the comparison of measured points and the lines calculated by Eq.(1) in Fig.15, Eq.(1) is a reasonably good description of the measured values. Now, let us shortly rationalize Eq.(1). When the wall thickness of the steel sample increases, its heat content increases with constant cooling area. Thus, when the sample is removed from the Zn-Mn bath of 450 °C, it takes a longer time for a thicker sample to cool down to the melting point of Zn. During this cooling period (while the Zn-Mn coating remains liquid), the Mn-atoms can diffuse with a high diffusion coefficient towards the surface (once the Zn-Mn layer is solidified, the diffusion coefficient of Mn through Zn drops by several orders of magnitude). The new Mn-atoms appearing at the Zn-Mn / ZnO layer react with the original ZnO-layer and convert it to MnO. Then, the Mn^{+2} ions diffuse through this MnO layer and thicken it at the MnO/air thanks to reaction with outer oxygen of air. The process is limited by the diffusion of Mn-atoms through the Zn-layer. That is why the MnO-thickness is proportional to the Mn-content in the zinc. It is possible only if the diffusion coefficient of Mn^{+2} ions through the MnO-layer is higher than the diffusion coefficient of Mn through liquid Zn. Unfortunately there are no data known in the literature for the diffusion coefficient of Mn^{+2} though MnO at 450 °C, so this hypothesis cannot be checked.

4.2. Modelling the critical Mn-content of liquid Zn

As follows from Eq.(1), MnO can appear on the surface of the galvanized sample only if $C_{(Mn(Zn))} > 0.025 \pm 0.010$ m/m%. This limiting value is probably due to thermodynamic limitation. In other words, it is probably the critical Mn content of Zn, being just sufficient to convert ZnO into MnO by the heterogeneous chemical reaction: $Mn + ZnO = MnO + Zn$.

According to the data of Barin [25], this chemical reaction is accompanied by the following standard Gibbs energy change at 450 °C: -53.8 ± 1.6 kJ/mol. Thus, the equilibrium constant of this reaction at 450 °C is: 5,900 ... 10,000. As all activities in the above reaction are approximately 1 except the activity of Mn in the Zn bath, the latter follows as the reciprocal of the equilibrium constant: $a_{Mn(Zn)} = (1.00 \dots 1.69) \cdot 10^{-4}$. This is the critical Mn-activity, above which Mn atoms dissolved in the Zn-bath can form MnO instead of the original ZnO on the top of liquid Zn at 450 °C.

Now, let us estimate the activity coefficient of Mn in infinite dilution in liquid Zn at 450 °C. Measured values are known only for the interaction energy in the binary Mn-Zn liquid alloy at 1573 K, being equal about -4.3 ± 0.5 kJ/mol [26]. This value is supported by measured values of [27], against the theoretical values of

Miedema [28]. This value can be re-calculated to 450 °C = 723 K using the exponential model and the fourth law (see [29-31]): -7.3 ± 0.8 kJ/mol. From here, the activity coefficient of Mn in infinitely diluted solution of liquid Zn at 450 °C follows as: 0.26 ... 0.34.

Dividing the above critical activity value by this activity coefficient value, the critical mole fraction of Mn in liquid Zn is found as: $(2.9 \dots 6.5) \cdot 10^{-4}$. This value can be converted into the critical m/m% of Mn in liquid Zn as: 0.024 ... 0.055. As this possible theoretical interval overlaps with the interval of empirical values $(0.025 \pm 0.010$ m/m% of Eq.(1), it is proven that the semi-empirical value of 0.025 ± 0.010 m/m% of Mn of Eq.(1) is approximately the critical minimum Mn-content in liquid Zn, ensuring that the original ZnO layer is converted to the MnO layer. As this critical value is below 0.1 m/m% Mn (which is the minimum Mn-content used in our experiments), therefore MnO was formed on the top of all samples, as proven by SNMS.

4.3. The relationship between the thickness of the MnO layer and the color of the sample

Combining the results shown in Table 4 and in Fig.15, both the sequence of colors (blue – yellow – pink – green) and the thickness of the oxide layer are similarly proportional to the Mn-content of the bath and to the steel thickness. Thus, it follows that the different colors of different steel samples shown in Figs. 4-12 are probably due to different thicknesses of the oxide (mostly MnO) layer on the top of the different samples.

To prove this hypothesis, the surface of one of the most coloured samples (see Fig.10, 0.2 m/m% Mn-content) was sputtered by Ar^+ ions for 70 s and for 140 s (see Fig.16). As a result, the original pink color turned into yellow color after 70 s of sputtering and turned into blue color after 140 s of sputtering. Thus, by sputtering the sample (i.e. gradually removing its top layer) the inverse sequence of the colors is reproduced as given above (pink – yellow – blue). This is because during sputtering the thickness of the MnO layer is gradually decreased, while during the galvanizing treatment of the samples the increasing Mn-content and the increasing steel-thickness leads to the increase in the oxide thickness. Thus, Fig.16 proves that the colors of the samples are indeed due to the thickness of the same oxide layer on their top.

4.4. The mechanism of coloring by the thin MnO layer

As was explained in our previous paper on laboratory experiments using Zn-Ti bath [23], coloring due to thin, transparent oxide layers (such as TiO_2 or MnO) are due to interference of natural light on these transparent thin oxides. The detailed theory and calculations are not repeated here. The interested reader can find the details in [23].





Figure 16. Photos of the sputtered by SNMS sample (Fig.10, 0.2 m/m% Mn) for 70 s (left) and for 140 s (right). See the color change in the circular sputtered spots.

5. Conclusions

Coloring hot dip galvanization was realized for 9 different steel samples in 3 different Zn-Mn baths in a large liquid bath containing 738 kg of Zn. The colors on the top of the Zn-Mn layer appear in a sequence of blue – yellow – pink – green as the Mn-content of the liquid Zn is increased or/and as the wall thickness of the steel plate is increased. The MnO layer identified on the top of the Zn-coating by SNMS. The top 10 nm of this MnO layer is contaminated by oxides of Si, Fe, Al and Mg (these metals originate from Zn, Mn and steel).

It is shown that the color of the samples is dependent on the thickness of the MnO layer, being due to the interference of natural light on this transparent MnO-nanolayer. The thickness of the MnO layer is described as function of the Mn-content of liquid Zn and the wall thickness of the steel sample. The thicker is the steel sample, the longer the solidification of the Zn layer takes, and thus there is longer time to thicken the outer MnO layer. The appearance of the MnO layer is possible only above the certain critical Mn-content of liquid Zn, being around 0.025 ± 0.010 m/m%. This value is found in agreement with the thermodynamic limit, when the dissolved Mn atoms can just convert the original ZnO layer on top of the galvanized coating into MnO.

Acknowledgements

The authors acknowledge the NAGEV Cink Ltd of Hungary, their management and people for providing us their production floor, production equipment and labour force to conduct our experiments. Additionally we are grateful to dr. Olivér Bánhidi (Institute of Chemistry, University of Miskolc) to perform ICP analysis of our Zn-Mn samples. This work was partly financed by the GINOP-2.3.2-15-2016-00027 project. SNMS measurements were carried out in frame of the GINOP-2.3.2-15-2016-00041 project.

References

- [1] A.R. Marder: Prog. Mater. Sci., 45 (2000) 191–271
- [2] A. Semoroz, L. Strezov, and M. Rappaz: Metall. Mater. Trans. A, 33A (2002) 695–701
- [3] A. Szabo, E. Denes: Mater. Sci. Forum 414-415 (2003) 45-50
- [4] F.M.Bellhouse, A.I.M.Mertense, J.R.McDermid: Mater. Sci. Eng. A. 463 (2007) 147-56
- [5] S.Kaboli, J.R.McDermid: Metall. Mater. Trans. A., 45A (2014) 3938 - 3953
- [6] H.Yang, S.Zhang, J.Li, Y.Liu, H.Wang: Surf. Coating Technol. 240 (2014) 269-274
- [7] S.M.A. Shibli, B.N.Meena, R.Remya: Surf. Coating Technol, 262 (2015) 210-215
- [8] G.Liu, J.Xing, S.Ma, Y.He, H.Fu, Y.Gao, Y.Wang, Y.Wang: Metall. Mater. Trans. A, 46 (2015) 1900-1907
- [9] Y.Wang, J.Zeng: Mater. Design: 69 (2015) 64-69
- [10] M.Panjan, M.Klanjsej Gunde, P.Panjan, M.Cekada: Surf. Coating Technol., 254 (2014) 65-72
- [11] J.Corredor, C.P.Bergmann, M.Pereira, L.F.P.Dick: Surf. Coating Technol. 245 (2014) 125-132.
- [12] D.P.Adams, R.D.Murphy, D.J.Saiz, D.A.Hirschfeld, M.A.Rodriguez, P.G.Kouta, B.H.Jared: Surf. Coating Technol., 248 (2014) 38-45.
- [13] R.W. Smyth: US patent 3530013, 1970
- [14] P. B. Philip, R. Zeliznak: US patent 3778315, 1971
- [15] M.Tomita, S.Yamamoto: European patent EP0269005A2, 1987
- [16] M.Tomita, S.Yamamoto, C. Tominaga, K. Nakayama: British patent GB1243562, 1991
- [17] Q. C. Le, J.Z. Cui: Chin. J. Nonferr. Met., 8 (1998) 98 - 102
- [18] Q. C. Le, J. Z. Cui: Acta Metall. Sin., 12 (1999) 1217-22
- [19] Q. C. Le, J.Z. Cui, C.H. Hou: Chin. J. Nonferr. Met., 10 (2000) 388- 94
- [20] Q.C. Le, J.Z. Cui: Surf. Eng., 24 (2008) 57-62
- [21] G. Lévai, M. Godzsák, A. Ender, R. Márkus, T.I. Török: Mater. Sci. Forum, 729 (2013) 61-67.
- [22] Y.Wang, J.Zheng: Surf. Coating Technol., 245 (2014) 55-65
- [23] G.Lévai, M.Godzsák, T.I.Török, J.Hakl, V.Takáts, A.Csik, K.Vad, G.Kaptay. Metall Mater Trans A, 47A (2016) 3580 – 3596.
- [24] C. Burattini, L. Zortea, F. Bisegna & S. Natali. Surf Eng, 33 (2017) 460-466.
- [25] I.Barin: Thermochemical Properties of Pure Substances, VCh, 1993, in 2 parts
- [26] I. Dimov, D. Nenov, N. Gidikova, A. Mosheva: Arch. Eisenhüttenwes. 48 (1977) 209–10.
- [27] E.H. Baker: Z.Metallkde 71 (1980) 760–762.
- [28] F.R. deBoer, R.Boom, W.C.M.Mattens, A.R.Miedema: Cohesion in Metals, North-Holland, Amsterdam, 1988.
- [29] G.Kaptay. Calphad 28 (2004) 115-124.
- [30] G.Kaptay. Metall Mater Trans A, 43A (2012) 531-543.
- [31] G.Kaptay. Calphad 56 (2017) 169-184.

